EBioMedicine 40 (2019) 528–540

Contents lists available at ScienceDirect

EBioMedicine

journal homepage: www.ebiomedicine.com

EBioMedicine
Published by THE LANCET

Targeting allosteric site of AKT by 5,7-dimethoxy-1,4-phenanthrenequinone suppresses neutrophilic inflammation

Po-Jen Chen [a,b], I-Ling Ko [b], Chia-Lin Lee [c,d], Hao-Chun Hu [e], Fang-Rong Chang [e], Yang-Chang Wu [e], Yann-Lii Leu [b,f,g], Chih-Ching Wu [h,i], Cheng-Yu Lin [b], Chang-Yu Pan [b], Yung-Fong Tsai [b,j], Tsong-Long Hwang [b,f,j,k,l,*]

[a] Department of Cosmetic Science, Providence University, Taichung 433, Taiwan
[b] Graduate Institute of Natural Products, College of Medicine, Chang Gung University, Taoyuan 333, Taiwan
[c] Chinese Medicine Research and Development Center, China Medical University Hospital, Taichung 404, Taiwan
[d] Department of Cosmeceutics, China Medical University, Taichung 404, Taiwan
[e] Graduate Institute of Natural Products, College of Pharmacy and Research Center for Natural Products & Drug Development, Kaohsiung Medical University, Kaohsiung 807, Taiwan
[f] Chinese Herbal Medicine Research Team, Healthy Aging Research Center, Chang Gung University, Taoyuan 333, Taiwan
[g] Center for Traditional Chinese Medicine, Chang Gung Memorial Hospital, Taoyuan 333, Taiwan
[h] Department of Medical Biotechnology and Laboratory Science, College of Medicine, Chang Gung University, Taoyuan 333, Taiwan
[i] Department of Otolaryngology – Head & Neck Surgery, Chang Gung Memorial Hospital, Taoyuan 333, Taiwan
[j] Department of Anaesthesiology, Chang Gung Memorial Hospital, Taoyuan 333, Taiwan
[k] Research Center for Chinese Herbal Medicine, Research Center for Food and Cosmetic Safety, Graduate Institute of Health Industry Technology, College of Human Ecology, Chang Gung University of Science and Technology, Taoyuan 333, Taiwan
[l] Department of Chemical Engineering, Ming Chi University of Technology, New Taipei City 243, Taiwan

ARTICLE INFO

Article history:
Received 21 December 2018
Received in revised form 22 January 2019
Accepted 22 January 2019
Available online 30 January 2019

Keywords:
Acute lung injury
AKT
5,7-dimethoxy-1,4-phenanthrenequinone
Inflammation
Neutrophil

ABSTRACT

Background: Acute lung injury (ALI) is a severe life-threatening inflammatory disease. Neutrophil activation is a major pathogenic factor in ALI. Protein kinase B (PKB)/AKT regulates diverse cellular responses, but the significance in neutrophilic inflammation and ALI remains unknown.
Methods: Human neutrophils and neutrophil-like differentiated HL-60 (dHL-60) cells were used to examine the anti-inflammatory effects of 5,7-dimethoxy-1,4-phenanthrenequinone (CLLV-1). The therapeutic potential of CLLV-1 was determined in a mouse model of lipopolysaccharide (LPS)-induced ALI.
Findings: CLLV-1 inhibited respiratory burst, degranulation, adhesion, and chemotaxis in human neutrophils and dHL-60 cells. CLLV-1 inhibited the phosphorylation of AKT (Thr308 and Ser473), but not of ERK, JNK, or p38. Furthermore, CLLV-1 blocked AKT activity and covalently reacted with AKT Cys310 *in vitro*. The $AKT_{309–313}$ peptide-CLLV-1 adducts were determined by NMR or mass spectrometry assay. The alkylation agent-conjugated AKT (reduced form) level was also inhibited by CLLV-1. Significantly, CLLV-1 ameliorated LPS-induced ALI, neutrophil infiltration, and AKT activation in mice.
Interpretation: Our results identify CLLV-1 as a covalent allosteric AKT inhibitor by targeting AKT Cys310. CLLV-1 shows potent anti-inflammatory activity in human neutrophils and LPS-induced mouse ALI. Our findings provide a mechanistic framework for redox modification of AKT that may serve as a novel pharmacological target to alleviate neutrophilic inflammation.

1. Introduction

Neutrophils are the first line of host defense in the innate immune response. They are chemoattracted to inflammatory regions in response to infection, and they subsequently eliminate invading pathogens through respiratory burst, degranulation, and neutrophil extracellular traps (NETs). However, overwhelming neutrophil activation plays a critical role both in infective and sterile inflammation [1–4]. The reactive oxygen species (ROS) and proteases released by activated neutrophils can damage healthy surrounding tissues, resulting in deleterious inflammatory lung diseases, such as acute lung injury (ALI), chronic obstructive pulmonary disease, or asthma [5–8].

Pathogen recognition or an inflammatory environment triggers many critical intracellular signal processes through surface receptors

* Corresponding author at: Graduate Institute of Natural Products, Chang Gung University, 259 Wen-Hwa 1st Road, Kweishan, Taoyuan 333, Taiwan.
E-mail address: htl@mail.cgu.edu.tw (T.-L. Hwang).

https://doi.org/10.1016/j.ebiom.2019.01.043

Research in context

Evidence before this study

Acute lung injury (ALI) is a severe life-threatening disease with high mortality. Neutrophil infiltration and activation play a critical role in ALI. Protein kinase B (PKB)/AKT controls diverse cellular responses. However, the role of AKT in regulating neutrophil functions is not well understood, and the targeting AKT for ALI remains unknown.

Added value of this study

We identify that 5,7-dimethoxy-1,4-phenanthrenequinone (CLLV-1) acts as a covalent allosteric AKT inhibitor by targeting AKT Cys310. CLLV-1 showed anti-inflammatory effects by suppressing neutrophil respiratory burst, degranulation, adhesion, and chemotaxis. Significantly, CLLV-1 ameliorated neutrophil infiltration, AKT activation, and lung injury in LPS-induced mouse ALI model. These results demonstrated that the targeting AKT in human neutrophils has the potential to treat ALI, and CLLV-1 may serve as a novel AKT inhibitor by targeting redox regulatory site of AKT.

Implications of all the available evidence

This study has provided evidences that AKT Cys310 is a pharmacological target for treating neutrophilic inflammatory diseases. CLLV-1 is a novel allosteric AKT inhibitor. CLLV-1 could act as a lead compound for treating ALI.

in neutrophils [9–12]. The serine/threonine-specific protein kinase, protein kinase B (PKB)/AKT, has been reported to regulate the neutrophil immune responses, including respiratory burst, degranulation, and chemotaxis [13–15]. In human neutrophils, activated AKT phosphorylates $p47^{phox}$, a component of nicotinamide adenosine dinucleotide phosphate (NADPH) oxidase, to initiate respiratory burst [16–18]. Pharmacological inhibition of phosphoinositide 3-kinase (PI3K)/AKT signaling reduces leukocyte degranulation [19,20]. AKT also stabilizes F-actin polymerization to enhance the chemotaxis of activated neutrophils [18,21,22]. Therefore, AKT may be a potential pharmacological target to treat neutrophilic inflammation. In addition to the well-known regulatory phosphorylation, AKT is inactivated through an intra-disulfide bond between Cys296 and Cys310 in the catalytic domain to cause misleading conformation along with dephosphorylation [23–26]. However, the mechanistic details of whether redox-controlled AKT activity contributes to neutrophilic inflammation remains to be explored.

In this study, we identified that 5,7-dimethoxy-1,4-phenanthrenequinone (CLLV-1) (Fig. 1a) is a AKT inhibitor *via* a redox reaction with the Cys310 residue of AKT to block its kinase activity. CLLV-1 has been shown to exhibit anti-cancer activity and anti-vascular cell migration effect [27,28]. However, the underlying mechanism and direct target of CLLV-1 are unknown. Here, we found that CLLV-1 has an anti-inflammatory potential to impede respiratory burst, degranulation, and chemotaxis in activated human neutrophils or neutrophil-like differentiated HL-60 (dHL-60) cells. Moreover, administration of CLLV-1 ameliorated the inflammatory lung injury in lipopolysaccharide (LPS)-induced ALI in mice. Our findings demonstrate that redox modification of AKT may be a novel pharmacological strategy for suppressing neutrophil-dominant lung disorders. We also suggest that CLLV-1 has the potential to be developed as an anti-inflammatory drug.

2. Materials and methods

2.1. Reagents

CLLV-1 was synthesized by Dr. Chia-Lin Lee, Dr. Fang-Rong Chang, and Dr. Yang-Chang Wu [28]. The CLLV-1 structure was determined by ^{1}H nuclear magnetic resonance (NMR) spectrum analysis (Fig. 6c). The purity of CLLV-1 was higher than 96% as determined by high-performance liquid chromatography. MK-2206 was purchased from Selleckchem (Houston, TX, USA). WKYMVm was purchased from Tocris Bioscience (Ellisville, MO, USA). FITC-labeled anti-CD11b, anti-Ly-6G, and anti-myeloperoxidase (MPO) antibodies were purchased from eBioscience (San Diego, CA, USA). The antibodies against p38 or $p47^{phox}$ and protein G beads were purchased from Santa Cruz Biotechnology (Santa Cruz, CA, USA). Anti-phospho-$p47^{phox}$ antibodies were purchased from Abcam (Cambridge, MA, USA). Anti-PIP3 antibodies were purchased from Echelon Biosciences (Salt Lake City, UT, USA). Nonradioactive AKT kinase assay kit, anti-Akt (pan), anti-phospho-Akt (Ser473), anti-phospho-Akt (Thr308), and other antibodies were purchased from Cell Signaling (Beverly, MA, USA). RPMI 1640, DMEM, L-glutamine, Antibiotic-Antimycotic, dihydrorhodamine 123 (DHR123), *N*-formyl-Nle-Leu-Phe-Nle-Tyr-Lys (fNLFNYK), Alexa Fluor 594 Phalloidin, and Hoechst 33342 were purchased from Thermo Fisher Scientific (Waltham, MA, USA). Fetal bovine serum (FBS) was purchased from Biological Industries (Beth Haemek, Israel). Other regents were purchased from Sigma-Aldrich (St. Louis, MO, USA).

2.2. Neutrophil isolation and cell culture

The procedure of neutrophil isolation was approved by the Institutional Review Board at Chang Gung Memorial Hospital. Neutrophils were isolated by dextran sedimentation and Ficoll-Hypaque centrifugation. Blood was obtained from healthy volunteers (20–35 years old), and written informed consent was obtained from every volunteer. The purified neutrophils contained >98% viable cells, determined by trypan blue exclusion assay [29].

bEnd.3 endothelial cells (ECs) were obtained from the Bioresource Collection and Research Centre (Hsinchu, Taiwan) and cultured in DMEM media supplemented with 10% FBS and 1× Antibiotic-Antimycotic. The human promyelocytic leukemic HL-60 cell line was purchased from ATCC and cultured in RPMI 1640 medium supplemented with 20% FBS, 2 mM L-glutamine, and 1× Antibiotic-Antimycotic. Both cell lines were grown in a humidified atmosphere (37 °C, 5% CO_2). The HL-60 cells were differentiated to neutrophil-like cells (dHL-60 cells) by a 5-day treatment with 1.3% DMSO in the growth medium.

2.3. Extracellular superoxide anion production

Human neutrophils (6×10^5 cells/mL) or dHL-60 cells (1×10^6 cells/mL) were equilibrated with 0.5 mg/mL ferricytochrome *c* and 1 mM Ca^{2+} at 37 °C for 5 min. The cells were then preincubated with DMSO, CLLV-1, or MK-2206 and stimulated with *N*-Formyl-Met-Leu-Phe (fMLF), sodium fluoride (NaF), or WKYMVm before being primed with cytochalasin B (CB; 1 or 2 μg/mL) for 3 min. The superoxide anion was determined using a spectrophotometer (Hitachi, Tokyo, Japan) at 550 nm.

2.4. Intracellular ROS formation

DHR123 (2 μM)-labeled human neutrophils or dHL-60 cells (1×10^6 cells/mL) were incubated at 37 °C for 10 min. Subsequently, the cells were pretreated with DMSO or CLLV-1 for 5 min and activated by fMLF (0.1 μM)/CB (1 μg/mL) for another 5 min. The intracellular ROS formation was determined using a flow cytometer (BD Bioscience).

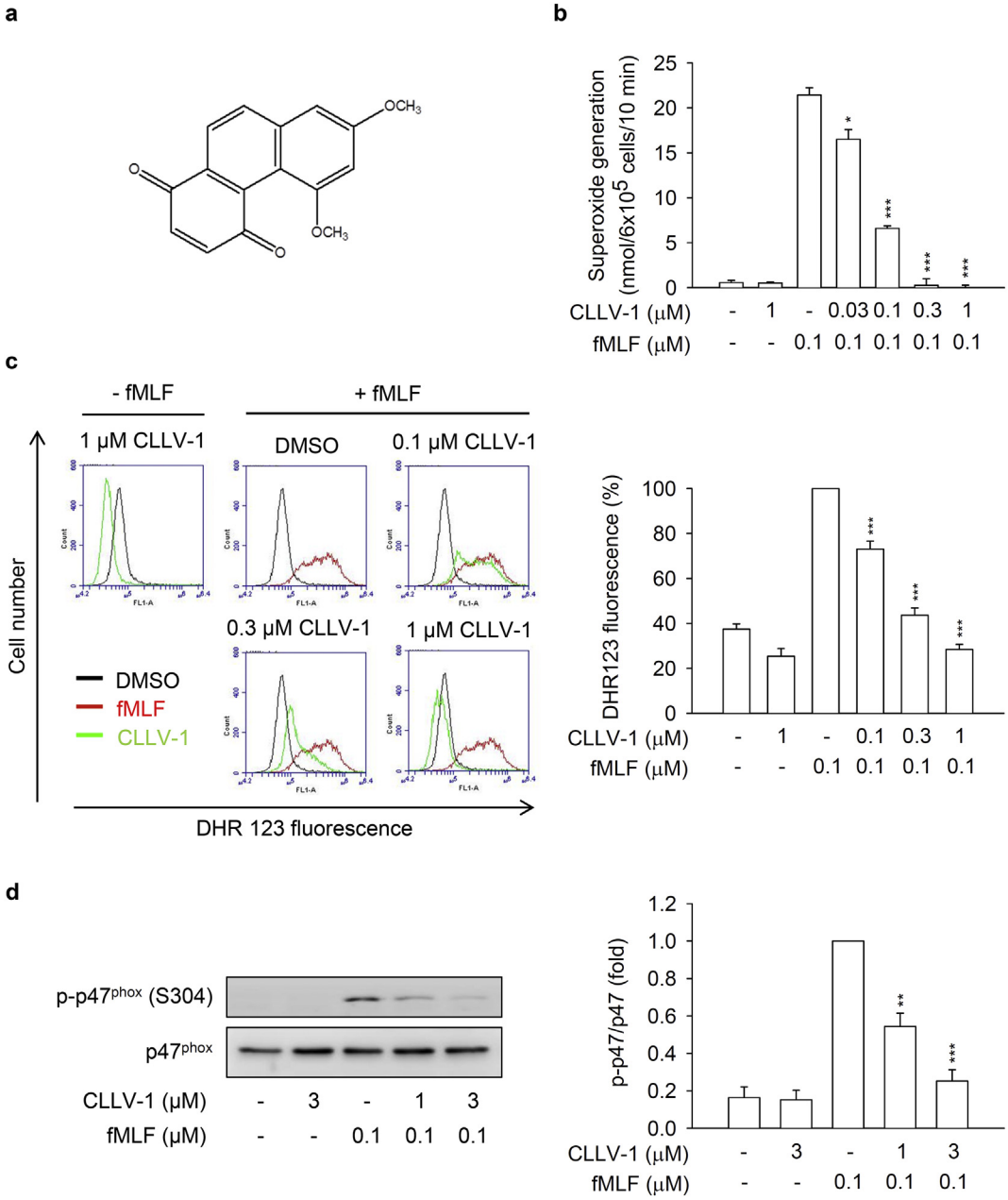

Fig. 1. CLLV-1 attenuates superoxide anion generation, ROS formation, and p47^{phox} phosphorylation in fMLF-activated human neutrophils. (a) The chemical structure of CLLV-1. (B–C) Human neutrophils were preincubated with DMSO or CLLV-1 (0.03–3 μM) and then activated with or without fMLF (0.1 μM)/CB (1 μg/mL). (b) Superoxide anion generation was detected using cytochrome *c* reduction by a spectrophotometer at 550 nm. (c) The intracellular ROS was monitored by flow cytometry, using cell-permeable DHR123. (d) Phosphorylation of p47^{phox} was analyzed by immunoblotting, using antibodies against the phosphorylated (S304) and total p47^{phox}. All data are expressed as mean values ± SEM ($n = 3$); $^{*}p < .05$, $^{**}p < .01$, and $^{***}p < .001$ compared with the DMSO + fMLF group (Student's *t*-test).

2.5. Elastase release

Human neutrophils (6×10^5 cells/mL) were equilibrated with an elastase substrate (MeO-Suc-Ala-Ala-Pro-Val-p-nitroanilide; 100 μM) at 37 °C for 5 min and then incubated with DMSO, CLLV-1, or MK-2206 for 5 min. The cells were then activated by fMLF, NaF, WKYMVm, interleukin-8 (IL-8), or leukotriene B4 (LTB_4) for a further 10 min. CB (0.5 or 2 μg/mL) was added 3 min before stimulation. Elastase release was determined by spectrophotometry at 405 nm.

2.6. CD11b expression

Neutrophils (5×10^6 cells/mL) were preincubated with DMSO or CLLV-1 for 5 min and activated by fMLF (0.1 μM)/CB (0.5 μg/mL) for another 5 min. The cell pellets were then resuspended in 5% bovine serum albumin (BSA) containing FITC-labeled anti-CD11b antibodies (1 μg) at 4 °C for 90 min. The fluorescence intensity was measured by flow cytometry.

2.7. Western blotting

Human neutrophils were preincubated with DMSO or CLLV-1 at 37 °C for 5 min and then activated by fMLF, NaF, WKYMVm, IL-8, or LTB_4 before being primed with CB. The reaction was stopped using the sample buffer (62.5 mM pH 6.8 Tris-HCl, 4% SDS, 5% β-mercaptoethanol, 2.5 mM Na_3VO_4, 0.00125% bromophenol blue, 10 mM di-N-pentyl phthalate, and 8.75% glycerol) at 100 °C for 15 min. The cell lysates were separated by sodium dodecyl sulfate (SDS)-polyacrylamide gel

electrophoresis (PAGE), and assayed by immunoblotting with the corresponding antibodies, followed by incubation with horseradish peroxidase-conjugated secondary anti-rabbit or anti-mouse antibodies. The labeled proteins were measured using an enhanced chemiluminescence system (Amersham Biosciences, Piscataway, NJ, USA).

2.8. Phosphatidylinositol (3,4,5)-trisphosphate (PIP3) and F-actin expression

Neutrophils or dHL-60 cells (5×10^6 cells/mL) were preincubated with DMSO or CLLV-1 for 5 min and then activated by fMLF (0.1 μM)/CB (1 μg/mL). The reaction was stopped by 4% paraformaldehyde at 25 °C for 20 min and then permeabilized with 0.1% Triton-X-100. For F-actin staining, cells were incubated with Alexa Fluor 594 Phalloidin in Hank's balanced salt solution (HBSS) containing 2% BSA at 25 °C for 60 min. For PIP3 expression, cells were incubated with anti-PIP3 antibodies and FITC-labeled anti-mouse IgG antibodies in HBSS containing 2% BSA at 25 °C for 60 min, respectively. The fluorescence intensity was monitored using flow cytometry.

2.9. AKT kinase assay

The AKT activity was determined using the non-radioactive AKT kinase assay kit according to the manufacturer's protocol. In brief, dHL-60 cells were activated by fMLF (0.1 μM)/CB (1 μg/mL), and the active AKT in the cell lysate was immunoprecipitated with immobilized AKT primary antibodies. The precipitated AKT was treated with DMSO, CLLV-1, or MK-2206 at 30 °C for 15 min and then incubated with ATP and GSK-3 fusion protein as a kinase substrate at 30 °C for 30 min. The reaction was stopped by 3 × SDS sample buffer at 100 °C for 5 min. The phosphorylation of the GSK-3 fusion protein was determined by western blot.

2.10. Molecular docking

CLLV-1 was docked on AKT proteins by docking optimization (CDOCKER) and optimized with the CHARMm force field using Discovery Studio 4.1 (DS) (BIOVIA, San Diego, CA). The binding of CLLV-1 and AKT1 with the most favorable energy was estimated with -CDOCKER (−kcal/mol). The crystal structure of AKT1 was obtained from the Protein Data Bank (PDB; accession code 4ekl). The 3D structure of CLLV-1 was drawn using ChemDraw Ultra 9.0.

2.11. NMR spectrum analysis

CLLV-1 (1 mg) or synthetic AKT peptides (1 mg) were dissolved in 0.5 mL DMSO *d6*. The mixtures of CLLV-1 (0.5 mg) and AKT peptides (1 mg) were vigorously mixed in 0.6 mL DMSO *d6* and incubated at 25 °C for 1 h. The ^{1}H NMR spectra were acquired using a Bruker AVANCE-400 MHz FT-NMR spectrometer (Bruker BioSpin GmbH, Billerica, MA).

2.12. Mass spectrometer (MS) analysis

Synthetic AKT peptides were dissolved in PBS. The mixtures of AKT peptides (120 μM) and CLLV-1 (60 μM) were incubated at 25 °C for 2 h. The AKT peptides and their CLLV-1 adducts were detected using matrix-assisted laser desorption/ionization time of flight mass spectrometer (MALDI-TOF MS). The AKT peptides and their CLLV-1 adducts were mixed with α-Cyano-4-hydroxycinnamic acid (CHCA) matrix (2 mg/mL in 80% acetonitrile containing 0.1% trichloroacetic acid) and loaded onto an MTP AnchorChip™ 600/384 TF (Bruker Daltonics GmbH, Bremen, Germany). After the crystallization of the peptides and the matrix, the samples were analyzed by an Ultraflex™ MALDI-TOF MS (Bruker Daltonics GmbH), controlled by the FlexControl software (v.2.2; Bruker Daltonics GmbH). Data processing was performed and monoisotopic peptide mass was acquired using the FlexAnalysis 2.4 peak-picking software (Bruker Daltonics GmbH).

2.13. 4-acetamido-4′-maleimidylstilbene-2,2′-disulfonic acid (AMS) labeling assay

The redox states of the proteins were examined by conjugating free thiol with AMS [23]. The cells were lysed in the buffer (50 mM Tris, pH 7.4, 150 mM NaCl, 0.5% Triton-X-100, and 1× protease inhibitor cocktail) and centrifuged at 12,000*g* for 10 min. The supernatants were incubated with 30 mM AMS at 4 °C for 24 h and then mixed with non-reducing sample buffer (62.5 mM pH 6.8 Tris-HCl, 4% SDS, 0.00125% bromophenol blue, and 8.75% glycerol) at 37 °C for 10 min. The redox states of the proteins were determined by immunoblotting.

2.14. Immunoprecipitation

Cells were lysed in the buffer (50 mM Tris, pH 7.4, 150 mM NaCl, 0.5% Triton X-100, 1× protease inhibitor cocktail) and centrifuged at 12,000*g* for 10 min. The supernatants were incubated with AKT antibodies bound to protein G beads. The beads were washed with buffer and the precipitated proteins were assayed by immunoblotting.

2.15. Neutrophil adhesion and chemotactic migration assays

The bEnd.3 ECs were activated with LPS (2 μg/mL) for 4 h. Hoechst 33342-labeled neutrophils were preincubated with DMSO or CLLV-1 for 5 min and activated by fMLF (0.1 μM)/CB (1 μg/mL) for another 5 min. Activated neutrophils were then co-cultured with LPS-pre-activated bEnd.3 ECs for 30 min. After gently washing, neutrophils adhering to bEnd.3 ECs were randomly counted in 4 fields by microscopy (IX81; Olympus, Center Valley, PA, USA) [29].

DMSO- or CLLV-1-pretreated neutrophils in the top microchemotaxis chamber (Merck Millipore, Darmstadt, Germany) were placed into the bottom well containing 0.1 μM fMLF. After 90 min, the migrated neutrophils were counted.

2.16. LPS-induced ALI

ALI was induced by intra-tracheal spray of 2 mg/kg LPS (*Escherichia coli* 0111:B4) in seven to eight weeks old C57BL/6 male mice, according to the guidelines and approved by Institutional Animal Care and Use Committee of Chang Gung University, Taiwan. Mice were fasted overnight and then intraperitoneally injected with CLLV-1 (10 mg/kg), MK-2206 (10 mg/kg) or an equal volume of DMSO (50 μl). After 1 h, tracheostomy was performed under anesthesia (30 mg/kg Zoletil 50 and 6 mg/kg xylazine). Mice were instilled with an intra-tracheal spray of 2 mg/kg LPS (dissolved in 40 μl 0.9% saline) or 0.9% saline and kept in a warm chamber to keep body temperature. After 6 h, the lungs were fixed in 10% formalin for immunohistochemistry or frozen for MPO activity.

2.17. MPO activity

The lung tissues were immersed in 10 mM PBS, pH 6.0, with 0.5% hexadecyltrimethylammonium bromide and sonicated by a homogenizer. The MPO activity was determined using MPO substrate buffer (PBS, pH 6.0, 0.2 mg/mL o-dianisidine hydrochloride, and 0.001% hydrogen peroxide) and monitored the absorbance at 405 nm by a spectrophotometer. The serial concentration of human MPO was used as a standard curve to calculate the MPO activity. Total protein levels were measured by the Bradford protein assay (Bio-Rad, Hercules, CA, USA). The final MPO activity was normalized to the corresponding protein concentration (U/mg).

2.18. Immunohistochemistry (IHC)

Formalin-fixed paraffin-embedded tissue sections were used for IHC. All slides were stained with hematoxylin and eosin (H&E) for morphologic determination. The anti-MPO antibodies, anti-Ly6G antibodies, anti-pAKT (S473) antibodies, or the SuperPicture kit (Thermo Fisher Scientific) were used as the primary or secondary antibodies, following a previously published protocol by Pathology Core of Chang Gung University [30].

2.19. Statistical analysis

Data are presented as means ± SEM. Statistical analysis was performed with SigmaPlot (Systat Software) using Student's *t*-test. $P < .05$ was considered statistically significant.

3. Results

3.1. CLLV-1 suppresses the inflammatory responses in fMLF-activated human neutrophils

To investigate the anti-inflammatory ability of CLLV-1, we first examined the effects of CLLV-1 on fMLF-induced respiratory burst, including superoxide anion production, ROS formation, and NADPH oxidase activation ($p47^{phox}$ phosphorylation) in human neutrophils. CLLV-1 dose-dependently inhibited superoxide anion generation and ROS formation with IC_{50} values of 0.058 ± 0.006 and 0.106 ± 0.022 μM, respectively (Fig. 1b and c). Importantly, it did not induce LDH release, suggesting that it did not cause membrane damage and cytotoxicity (Fig. S1a). We further evaluated how CLLV-1 inhibited the superoxide anion generation in fMLF-activated human neutrophils. In a cell-free xanthine/xanthine oxidase system, CLLV-1 (0.1–3 μM) did not exhibit a superoxide anion-scavenging ability. Superoxide dismutase (SOD) was a positive control. Superoxide anion is produced by NADPH oxidase in human neutrophils [17]. The isolated neutrophil membrane and cytosol fractions were used to examine the inhibitory effect of CLLV-1 on NADPH oxidase: CLLV-1 (0.3 and 3 μM) did not reduce superoxide anion production in SDS-reconstituted NADPH oxidase. Diphenyleneiodonium (DPI; 10 μM), an NADPH oxidase inhibitor, was a positive control (Fig. S1b-c). The phosphorylation of $p47^{phox}$, a component of NADPH oxidase, was repressed by CLLV-1 in fMLF-activated human neutrophils (Fig. 1d), suggesting that the anti-inflammatory effect of CLLV-1 on respiratory burst may be through modulating upstream signaling of NADPH oxidase in human neutrophils.

Next, the effects of CLLV-1 on human neutrophil degranulation and chemotaxis were determined. CLLV-1 repressed fMLF-induced elastase release with an IC_{50} value of 0.172 ± 0.011 μM (Fig. 2a). In contrast, it failed to alter the activity of elastase in a cell-free assay (Fig. S1d), suggesting that it inhibited human neutrophil degranulation *via* the regulation of intracellular signaling pathways. In addition, integrin CD11b activation leads to neutrophils adhering to endothelial cells and subsequently induces neutrophil migration and infiltration. F-actin polymerization at the leading edge in polarized neutrophils governs the chemotaxis [22]. CLLV-1 decreased CD11b expression and F-actin assembly in fMLF-activated human neutrophils and suppressed fMLF-induced neutrophil adhesion to bEnd.3 ECs and migration (Fig. 2b-e and Fig. S2). Together, CLLV-1 exhibits an anti-inflammatory potential to alleviate neutrophilic inflammation, including respiratory burst, degranulation, and chemotaxis.

3.2. CLLV-1 ameliorates AKT activation in response to various stimuli in human neutrophils

This study aimed to identify the target protein of CLLV-1 in human neutrophils. The fMLF mainly binds to formyl peptide receptor 1 (FPR1) to activate neutrophils through multiple intracellular signaling pathways such as AKT and mitogen-activated protein kinases (MAPKs) [31,32]. CLLV-1 (0.1–3 μM) did not compete with the fluorescently labeled fMLF analog fNLFNYK for FPR1 binding (Fig. S1e), ruling out the effect of CLLV-1 on FPR1. Therefore, the activation of AKT, ERK, JNK, and p38 was examined in fMLF-activated human neutrophils. CLLV-1 inhibited the phosphorylation of AKT (Thr308 and Ser473), but not of ERK, JNK, or p38 (Fig. 3). Because CLLV-1 selectively restrained AKT activation, we wondered whether CLLV-1 suppressed AKT activation and inflammatory responses in different stimuli-activated human neutrophils, including NaF (direct G protein activator), WKYMVm (FPR2 agonist), IL-8, and LTB_4 [33]. Further, CLLV-1 significantly inhibited NaF- and WKYMVm-induced superoxide anion generation in human neutrophils. It also showed an inhibitory effect on elastase release in NaF-, WKYMVm-, IL-8-, and LTB_4-activated human neutrophils (Fig. S3). Notably, it significantly suppressed the activation of AKT in human neutrophils activated by all tested stimuli (Fig. S4), suggesting that AKT may be the target of CLLV-1 in human neutrophils. Another potent AKT inhibitor, MK-2206 [34], also inhibited the superoxide anion generation and elastase release in fMLF-activated human neutrophils (Fig. S5), supporting that inhibition of AKT is a potential strategy to attenuate neutrophilic inflammation.

3.3. CLLV-1 inhibits the inflammatory responses and AKT activation in fMLF-activated dHL-60 cells

HL-60 cells were exposure to DMSO for 5 days to differentiate into neutrophil-like cells (dHL-60 cells). Usage of dHL-60 cells provided enough cells for several biochemical experiments instead of limited primary human neutrophils. The increased FPR1 expression and cellular morphology of dHL-60 were observed to represent the neutrophil-like status (Fig. S6). CLLV-1 diminished superoxide anion generation and intracellular ROS formation in fMLF-induced dHL-60 cells. It also repressed the $p47^{phox}$ phosphorylation and F-actin polymerization in fMLF-activated dHL-60 cells (Fig. S7), suggesting that dHL-60 cells provide a good inflammatory model and that CLLV-1 still restrains the respiratory burst and chemotaxis in fMLF-activated dHL-60 cells. Importantly, CLLV-1 also attenuated fMLF-induced activation of AKT in dHL-60 (Fig. 4f).

3.4. CLLV-1 directly alleviates AKT activity

We tested whether the CLLV-1-inhibited AKT activation is based on altering the upstream kinases of AKT, including phosphoinositide-dependent protein kinase 1 (PDK1), mammalian target of rapamycin C2 (mTORC2), and PI3K [35,36]. CLLV-1 (0.3–3 μM) failed to affect the phosphorylation of PDK1 (S241), mTORC2 (S2481), and PI3K (Y199 of p85 subunit) in fMLF-activated dHL-60 cells and human neutrophils (Fig. 5a and Fig. S8). The level of PI3K-generated PIP3 was also not changed by CLLV-1 in fMLF-activated dHL-60 cells (Fig. 5b and Fig. S7c). Protein kinase A (PKA) has been shown to attenuate neutrophilic inflammation through inhibiting AKT activation [37,38]. However, CLLV-1 did not increase the level of cAMP. The PKA inhibitor, H89, did not reverse the CLLV-1-inhibited superoxide anion generation and elastase release in activated human neutrophils (Fig. S9).

We suggest that CLLV-1 may directly target AKT *per se* to repress inflammation in human neutrophils. To explore this hypothesis, the non-radioactive AKT kinase assay was performed *in vitro*. Clearly, our data showed that CLLV-1 (0.3–3 μM) blocked the kinase activity of AKT *in vitro*. MK-2206 was used as a positive control to inhibit AKT activity (Fig. 5 and Fig. S5c). Therefore, CLLV-1 acts as a novel AKT inhibitor to restrict the enzymatic activity of AKT.

3.5. CLLV-1 covalently reacts with AKT Cys310

To determine how CLLV-1 blocked the AKT activity, the molecular docking of CLLV-1 with AKT was performed. Based on CDOCKER and

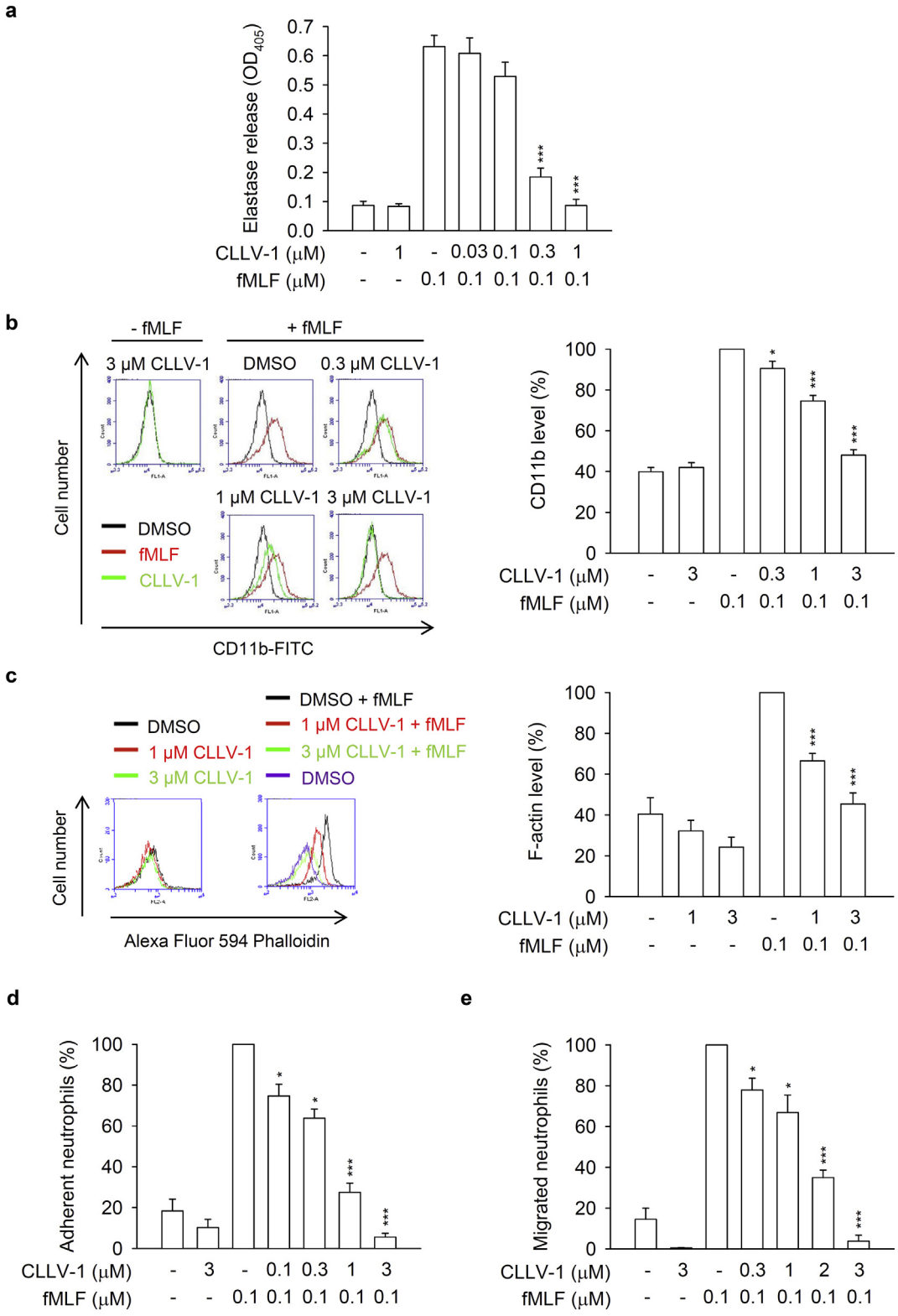

Fig. 2. CLLV-1 inhibits elastase release, CD11b/F-actin expression, and neutrophil adhesion/migration in fMLF-activated human neutrophils. (a-c) Human neutrophils were incubated with DMSO or CLLV-1 (0.3–3 μM) for 5 min before stimulation with or without fMLF (0.1 μM)/CB (0.5 or 1 μg/mL). (a) Elastase release was measured by a spectrophotometer at 405 nm, using elastase substrate. (b) The CD11b levels on cell surface were detected by flow cytometry, using FITC-labeled anti-CD11b antibodies. (c) The F-actin levels were assayed by flow cytometry, using Alexa Fluor 594 Phalloidin. (d) Hoechst 33342-labeled neutrophils were pretreated with DMSO or CLLV-1 (0.1–3 μM) for 5 min and stimulated with fMLF (0.1 μM)/CB (1 μg/mL). Sequentially, neutrophils were incubated with LPS-preactivated ECs for another 30 min. After gently washing, EC-associated neutrophils were counted under a microscope. (e) Neutrophils were preincubated with DMSO or CLLV-1 (0.3–3 μM) for 5 min in the top chamber. Migrated neutrophils in the bottom wells with or without fMLF were counted after 90 min. All data are expressed as mean values ± SEM ($n = 3$); *$p < .05$, **$p < .01$, and ***$p < .001$ compared with the DMSO + fMLF group (Student's t-test).

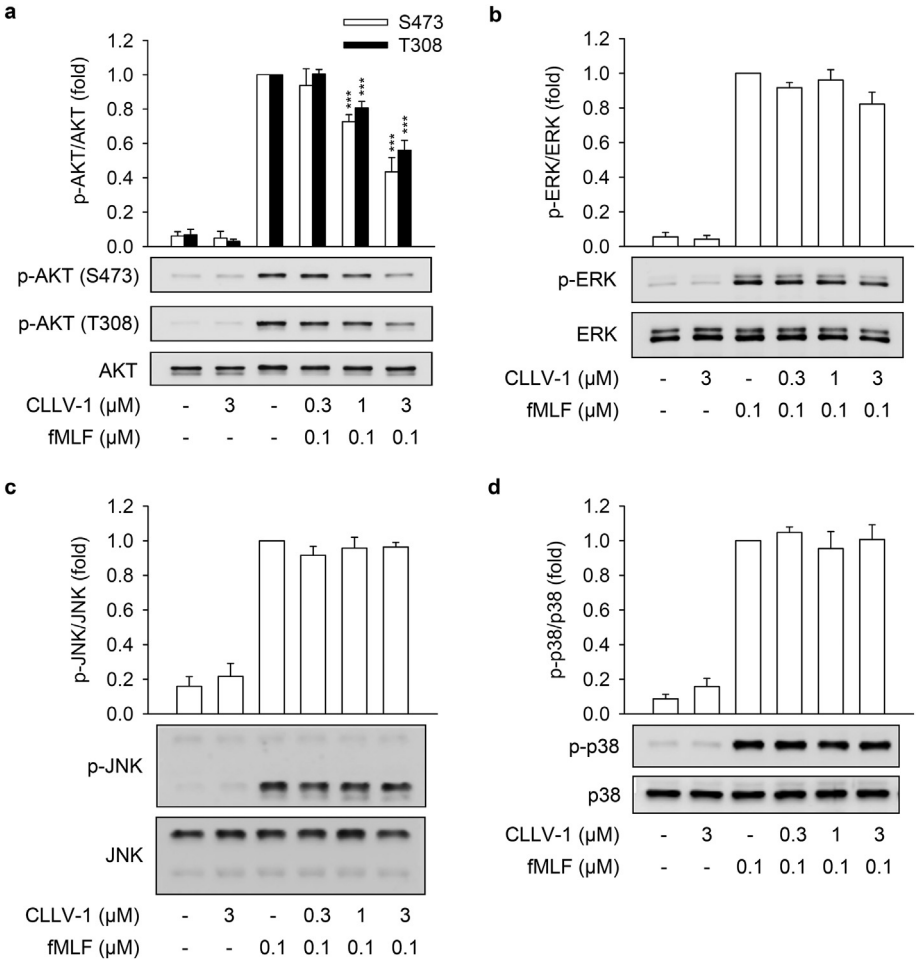

Fig. 3. CLLV-1 decreases the phosphorylation of AKT but not MAPKs in fMLF-activated human neutrophils. Human neutrophils were incubated with CLLV-1 (0.3–3 μM) for 5 min before stimulation with or without fMLF (0.1 μM)/CB (1 μg/mL). Phosphorylation of (a) AKT, (b) ERK, (c) JNK, or (d) p38 MAPK was analyzed by immunoblotting using antibodies against the phosphorylated form and the total of each protein. All data are expressed as mean values ± SEM (n = 3); ***$p < .001$ compared with the DMSO + fMLF group (Student's *t*-test).

the CHARMm force field, the CLLV-1-AKT binding modes were generated in receptor cavities with 10 poses. The binding of CLLV-1 and AKT with the most favorable energy was estimated with -CDOCKER (−474.532 kcal/mol). The *p*-benzoquinone, aromatic ring, or carboxyl group of CLLV-1 were proposed to interact with the R273, D274, L275, C310, G311, A317, L316, Y315, V320, or V330 residues of AKT (Fig. 6a–b), suggesting that CLLV-1 may preferably and specifically associate with this proposed "pocket" of AKT. Interestingly, the Cys310 residue of AKT was appeared in the predicted CLLV-1-binding site, and the redox modification of Cys310 in AKT is important for AKT enzymatic activity [23,39]. Hence, CLLV-1 may bind to the thiol group of Cys310 to interfere with the AKT activity. To address this hypothesis, the reaction between CLLV-1 and synthetic AKT peptides, $AKT_{304–308}$ (ATMKT), $AKT_{309–313}$ (FCGTP), $AKT_{314–318}$ (EYLAP), and $AKT_{307–328}$ (KTFCGTPEYLAPEVLEDNDYGR) were determined by NMR or MS (Fig. 6c–e): CLLV-1 covalently reacted with the $AKT_{309–313}$, exhibiting a new singlet peak at δ 7.00, but did not react with the adjacent $AKT_{304–308}$ and $AKT_{314–318}$, which lacked cysteine residues according to the ^{1}H NMR analysis (Fig. S10a). The AKT peptide-CLLV-1 adducts were also examined by MS (Fig. S10b): the molecular masses of $AKT_{309–313}$, $AKT_{307–328}$, and CLLV-1 were 524, 2389, and 268 Da, respectively. If CLLV-1 reacted with the AKT peptides, the proposed molecular masses of the adducts would be 792 Da ($AKT_{309–313}$-CLLV-1) and 2657 Da ($AKT_{307–328}$-CLLV-1). The corresponding signals were observed by MS, including $AKT_{309–313}$ ($[M + H]^+$; 524.079), $AKT_{307–328}$ ($[M + H]^+$; 2389.124), $AKT_{309–313}$-CLLV-1 ($[M_{CLL} + H]^+$; 792.244), and $AKT_{307–328}$-CLLV-1 ($[M_{CLL} + H]^+$; 2655.102). In addition, the sodium adducts (plus 23 Da) were also found, $AKT_{309–313}$-Na ($[M + Na]^+$; 546.145), $AKT_{307–328}$-Na ($[M + Na]^+$; 2411.258), and $AKT_{309–313}$-CLLV-1-Na ($[M_{CLL} + Na]^+$; 812.264). Similarly, the results of MS confirmed that CLLV-1 did not react with the adjacent peptides $AKT_{304–308}$ and $AKT_{314–318}$, which do not contain Cys310. These results suggested that CLLV-1 covalently reacted with Cys310 in AKT *via* an electrophilic addition.

To confirm the effect of CLLV-1 on AKT redox status in cells, we used the alkylation agent, AMS, to label reduced form of protein along with increasing molecular weight [23]. The level of AMS-labeled AKT (reduced form) was increased in fMLF-activated dHL-60 cells. CLLV-1 (0.3–3 μM) dose-dependently decreased the levels of AMS-labeled AKT in fMLF-activated dHL-60 cells (Fig. 7a). It has been reported that oxidization of Cys310 residue in AKT diminished its enzymatic activity and increased the AKT-protein phosphatase 2A (PP2A) interaction along with inhibition of AKT phosphorylation [23,24]. CLLV-1 induced the AKT-PP2A interaction in fMLF-activated dHL-60 cells (Fig. 7b). These results suggest that CLLV-1 covalently targets Cys310 of AKT to alleviate AKT activity as well as phosphorylation.

3.6. CLLV-1 attenuates LPS-induced ALI in mice

LPS/endotoxin is a critical pathogen to trigger ALI [40,41]. However, the role of AKT as a potential drug target in ALI needs to be studied. To examine the anti-inflammatory potential of CLLV-1 *in vivo*, the protective effects of CLLV-1 on LPS-induced ALI was tested in mice. Intratracheal instillation of LPS showed an increase in pulmonary

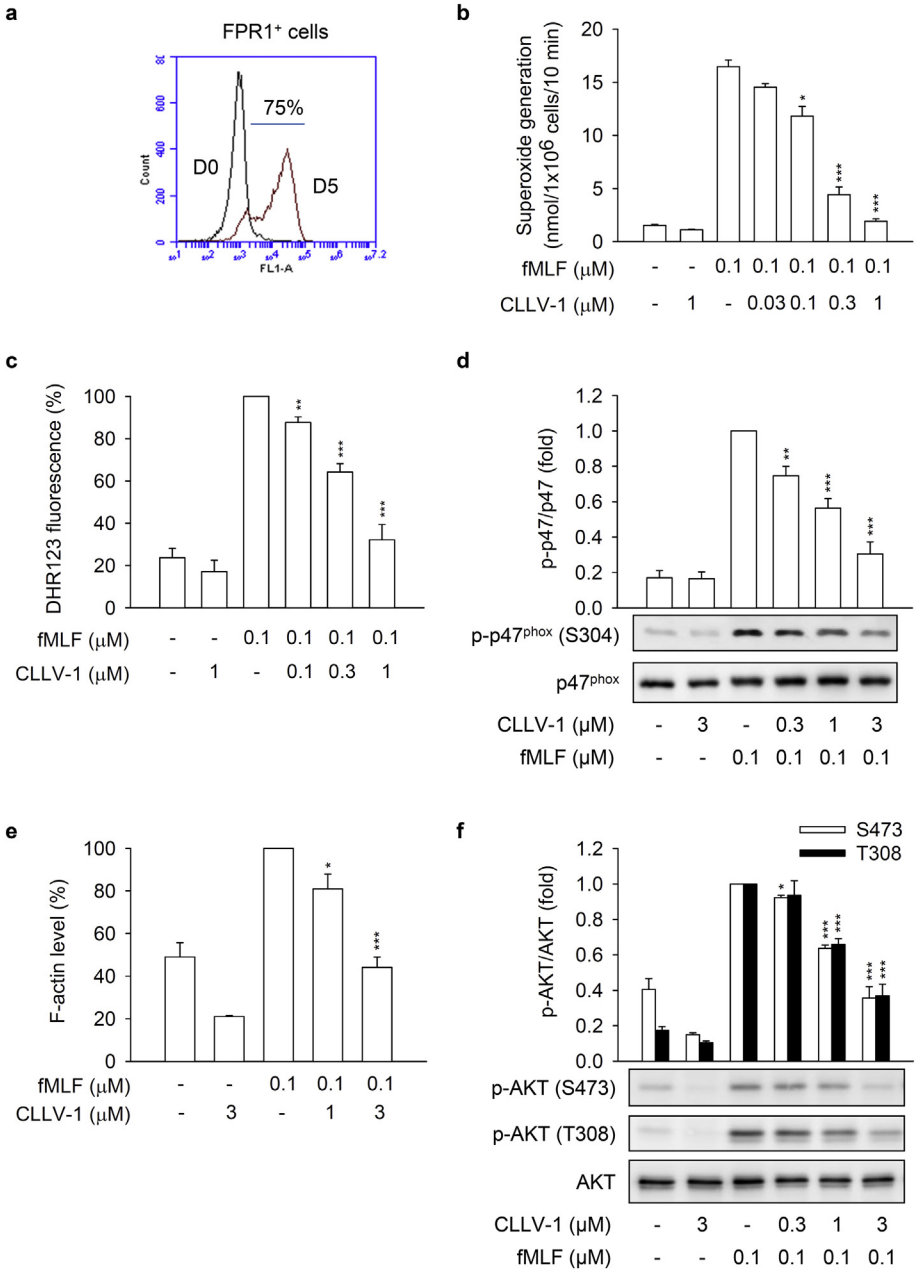

Fig. 4. CLLV-1 suppresses fMLF-induced inflammatory responses in differentiated HL-60 (dHL-60) cells. (a) The HL-60 cells were exposed to 1.3% DMSO for 5 days. The differentiation of HL-60 cells by DMSO was examined by flow cytometry, using anti-FPR1 antibodies. (B–F) The dHL-60 cells were preincubated with DMSO or CLLV-1 (0.03–1 μM) and then activated with or without fMLF (0.1 μM)/CB (1 μg/mL). (b) Superoxide anion generation was detected by spectrophotometry at 550 nm, using cytochrome *c* reduction. (c) The intracellular ROS was monitored by flow cytometry, using cell-permeable DHR123. (d) Phosphorylation of $p47^{phox}$ was analyzed by immunoblotting, using antibodies against the phosphorylated (S304) and total $p47^{phox}$. (e) F-actin levels were assayed by flow cytometry, using Alexa Fluor 594 Phalloidin. (f) Phosphorylation of AKT was analyzed by immunoblotting, using antibodies against the phosphorylated (S473 and T308) and total AKT. All data are expressed as mean values ± SEM (n = 3); $^{*}p < .05$, $^{**}p < .01$, and $^{***}p < .001$ compared with the DMSO + fMLF group (Student's *t*-test).

MPO, which was inhibited by intraperitoneal injection of CLLV-1 (10 mg/kg) or MK-2206 (10 mg/kg) (Fig. 8a). The total protein levels were measured to represent the severity of pulmonary edema. Both CLLV-1 and MK-2206 effectively attenuated the LPS-induced increase of protein levels in the lungs (Fig. 8b). The histopathological features of the lungs showed that LPS triggered inflammatory cell infiltration, inter-alveolar septal thickening, and interstitial edema. Moreover, LPS induced the infiltration of cells positive for Ly6G, a specific neutrophil marker, as well as AKT activation in the lungs. Noticeably, administration of CLLV-1 and MK-2206 ameliorated LPS-induced distortion of pulmonary architecture, Ly6G-positive infiltrated neutrophils, and AKT phosphorylation (Fig. 8c), suggesting the therapeutic potential of CLLV-1 in neutrophil-dominant lung diseases. Together, CLLV-1 and MK-2206 successfully impeded the inflammatory ALI *in vivo*, supporting that pharmacologically targeting redox modification of AKT is a potential strategy for treating neutrophilic lung injury.

4. Discussion

Neutrophils play a significant role in innate immunity; however, enhanced ROS generation and protease release by activated neutrophils can cause cell and tissue damage [5,42]. Neutrophilic inflammation has been found to play a central role in the pathogenesis of ALI/acute respiratory distress syndrome (ARDS). The AKT pathway is known to be involved in many neutrophil responses, including respiratory burst, degranulation, and chemotaxis [13–15,43]. However, the regulatory

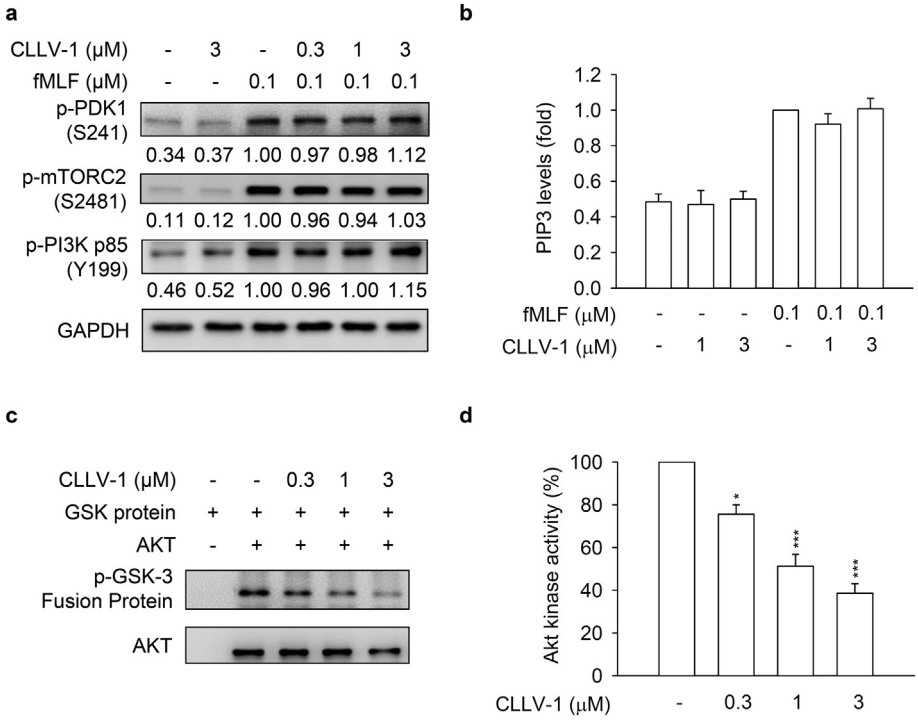

Fig. 5. CLLV-1 blocks AKT enzymatic activity but does not affect the AKT upstream kinases. (A-B) dHL-60 cells were preincubated with DMSO or CLLV-1 (0.03–1 μM) and then activated with or without fMLF (0.1 μM)/CB (1 μg/mL). (a) Phosphorylation of AKT upstream kinases, PDK1, mTORC2, and PI3K was determined by immunoblotting, using antibodies against the phosphorylated form and normalized to GAPDH. (b) PIP3 levels were assayed using anti-PIP3 antibodies by flow cytometry. (c) The active AKT proteins were immunoprecipitated using anti-phospho-AKT antibodies and treated with DMSO or CLLV-1 (0.3–3 μM) for 15 min at 30 °C. Subsequently, the GSK-3 fusion protein (AKT substrate) was added for another 30 min. The phospho-GSK-3 fusion protein was examined by immunoblotting. (d) The phosphorylation of the GSK-3 fusion protein was quantified and expressed as a percentage to represent AKT activity. All data are expressed as mean values ± SEM (n = 3); $^{*}p < .05$ and $^{***}p < .001$ compared with the DMSO + AKT group (Student's *t*-test).

mechanisms of AKT in human neutrophils are still elusory. Furthermore, the potential of AKT as a therapeutic target in ALI remains unknown. Herein, we show that a synthetic phenanthrenequinone compound, CLLV-1, inhibits inflammatory responses in human neutrophils or neutrophil-like dHL-60 cells triggered by various stimuli. CLLV-1 selectively blocked AKT activity through covalently targeting the Cys310 residue of AKT. Moreover, CLLV-1 attenuated the inflammatory responses in LPS-induced ALI in mice, indicating that it is a potential anti-inflammatory compound and providing an example of disruption of the redox modulation of AKT for treating neutrophil-dominant lung diseases.

AKT-mediated cellular signaling is significantly responsible for inflammatory responses in neutrophils [13,14]. With stimulation, AKT translocated to the leading edge in polarized neutrophils and induced $p47^{phox}$ phosphorylation and F-actin polymerization to trigger respiratory burst and chemotaxis in neutrophils, respectively [17,18,21]. It may be a preferentially remedial strategy to ameliorate the overwhelming neutrophilic inflammation *via* pharmacologically targeting of AKT. In the present study, we identified that CLLV-1 significantly abrogated AKT activation in response to various stimuli in human neutrophils (Fig. 3 and S4). As well, CLLV-1 dose-dependently restricted AKT-mediated $p47^{phox}$ phosphorylation and F-actin levels in activated human neutrophils and dHL-60 cells (Figs. 1, 2, and 4), confirming that CLLV-1-inhibited AKT activation is critical for halting inflammatory activation in human neutrophils.

AKT is composed of the pleckstrin homology (PH), catalytic kinase, and regulatory domains and its kinase activity is regulated through conformational dynamics. With stimulation, AKT is phosphorylated at Thr308 and Ser473 residues, leading to the PH domain becoming more distant from the kinase domain as "active" form. When AKT is dephosphorylated by PP2A, the catalytic domain would be interfered by more closed PH domain as "inactive" form [35,36]. Thus far, emerging evidence has supported the important role of redox modification of AKT in conformational dynamics [25]. An intramolecular disulfide bond between Cys296 and Cys310 in the catalytic domain of AKT that prompts dephosphorylation by associating with PP2A has been identified; oxidized and dephosphorylated AKT is considered to have lost its kinase activity [23,24,39]. In the present study, we found that CLLV-1 covalently reacted with Cys310 of AKT *in vitro* and repressed the alkylation agent-labeled AKT levels (reduced form) in cells (Figs. 6 and 7), supporting that CLLV-1 brings about AKT oxidation. The AKT-PP2A interaction was also increased by CLLV-1 along with dephosphorylation of AKT (Fig.7b) that was not modulated through AKT upstream kinases, including PDK1, mTORC2, and PI3K (Fig. 5a-b). Accordingly, CLLV-1-blocked AKT kinase activity may be dependent on redox modification of AKT.

CLLV-1 was proposed to interact with Cys310 of AKT by the molecular docking model (Fig. 6a–b). The adduct of $AKT_{309–313}$ peptides and CLLV-1 exhibited a new singlet peak at δ 7.00 in the ^{1}H NMR spectrum (Fig. 6c). The molecular masses of AKT peptide-CLLV-1 adducts (AKT peptide + CLLV-1 – $2H^{+}$ Da) were also detected in MALDI-TOF MS, $AKT_{309–313}$-CLLV-1-Na, and $AKT_{307–328}$-CLLV-1 (Fig. 6d-e), suggesting that the reaction between AKT and CLLV-1 is an electrophilic addition. It has been reported that thiol-based association between electrophilic compounds and proteins possessed selectivity and specificity. The structural characteristic of proteins and stereochemical structures of electrophiles results in their targeting selectivity [44,45]. The redox modulations of ERK, JNK, or p38 have been characterized in response to intracellular ROS. The cysteines of ERK2 (Cys38 and Cys214), JNK2 (Cys41) and p38 (Cys162) are responsible for their activity and phosphorylation [25,46,47]. However, CLLV-1 only repressed AKT, but not ERK, JNK, or p38 activation in human neutrophils (Fig. 3), implying its specificity. Using molecular docking model, the most favorable CLLV-1-binding pocket of AKT was determined, including R273, D274, L275, C310, G311, A317, L316, Y315, V320, or V330 residues (Fig. 6a–b). Importantly, another critical Cys296 of catalytic region was not proposed

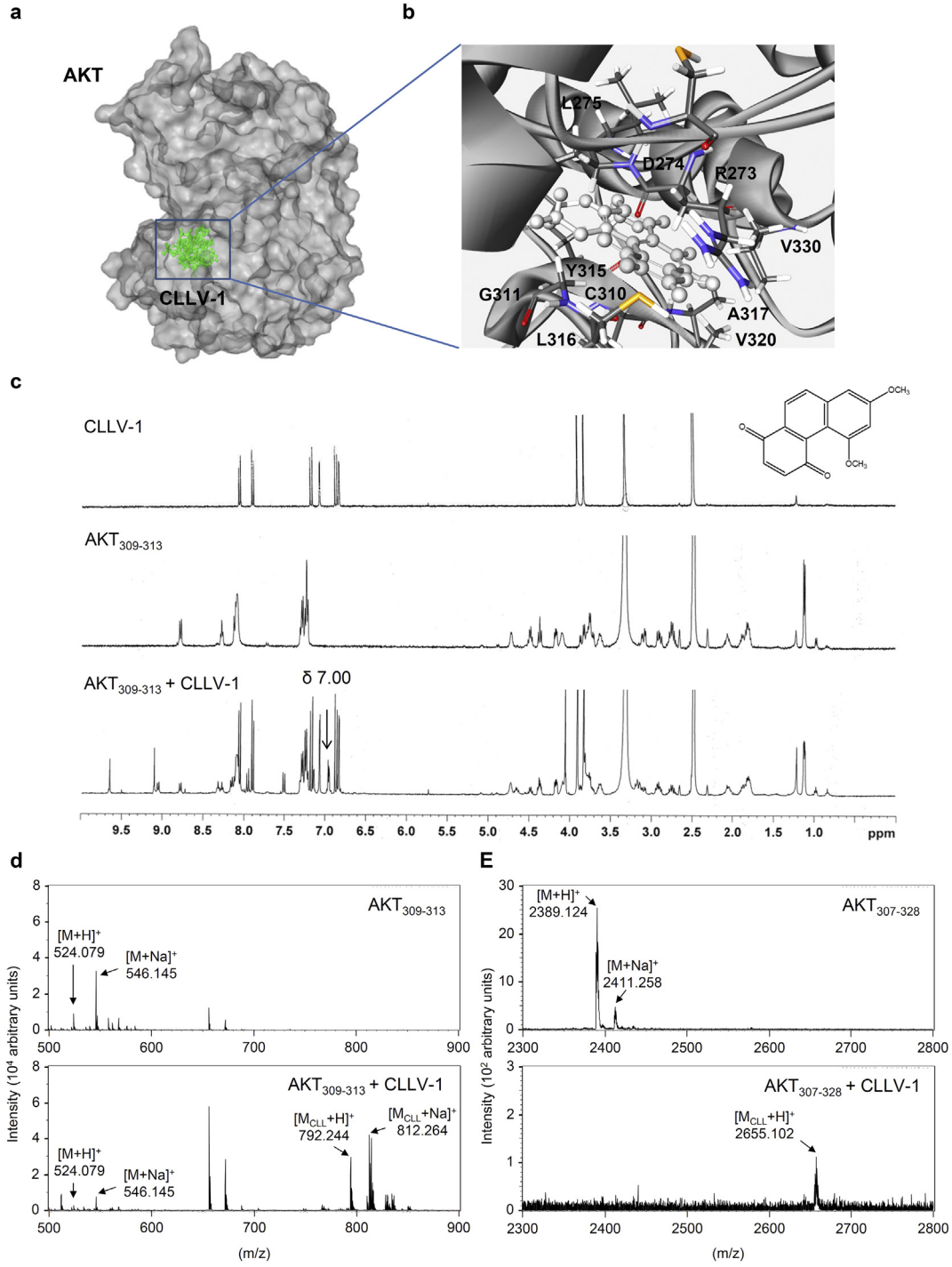

Fig. 6. CLLV-1 covalently reacts with the thiol group of an AKT cysteine *in vitro*. (a-b) Docking models of CLLV-1-targeted AKT. Surface presentation demonstrates the structure of AKT (gray). CLLV-1 moieties are colored green and rendered in stick representation (a). Close-up of CLLV-1 docking site (best energy mode) (b). The figures were prepared using Discovery Studio 4.1. The crystal structure of AKT was downloaded from PDB (accession code 4ekl). The chemical structure of CLLV-1 was drawn by ChemDraw Ultra 9.0. (c) ^{1}H NMR spectra of CLLV-1 (upper panel), synthetic AKT peptide ($AKT_{309–313}$; FCGTP) (middle panel), and mixtures of CLLV-1 and $AKT_{309–313}$ (lower panel). (d-e) The synthetic AKT peptides $AKT_{309–313}$ and $AKT_{307–328}$ (KTFCGTPEYLAPEVLEDNDYGR) were incubated in the presence or absence of CLLV-1. The molecular mass of the synthetic AKT peptides and their CLLV-1 adducts were detected using MALDI-TOF MS. M, molecular mass of AKT peptides; M_{CLL}, molecular mass of adducts of AKT peptides and CLLV-1.

as CLLV-1-targeting site (data not shown), suggesting that CLLV-1 exhibits target-site selectivity in AKT.

Developed AKT inhibitors are classified as ATP-competitive and allosteric inhibitors [48,49]. However, the off-target effect of ATP-competitive inhibitors is still of concern because of the ATP-binding site being highly conserved among members of the AGC kinase family such as PKA and PKC [50]. A growing number of allosteric inhibitors with higher efficacy and specificity, such as MK-2206, are being developed [34]. Recently, the development of structure-based covalent-allosteric AKT inhibitors has been mentioned because of their high potency and selectivity to stabilize AKT as inactive conformation [51,52]. The Cys296 and Cys310 residues in the catalytic domain of AKT were identified as allosteric sites for regulating AKT activity [49,53,54]. Therefore, the Cys296 and Cys310 residues of AKT are potential therapeutic

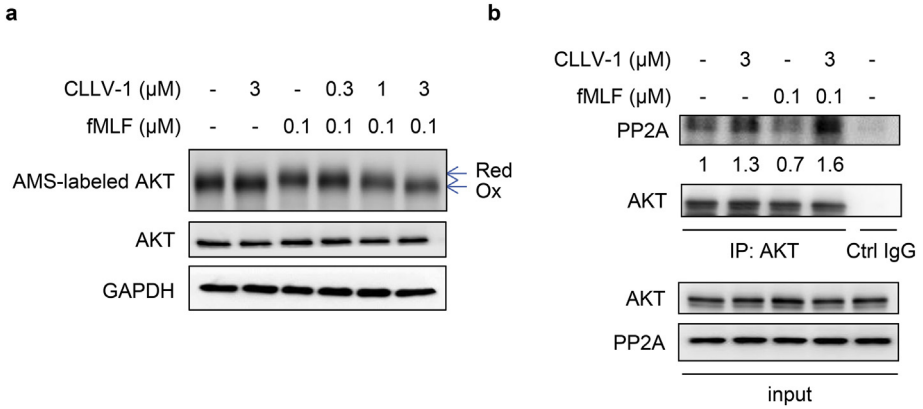

Fig. 7. CLLV-1 decreases the AMS-labeled reduced form of AKT and increases the AKT-PP2A interaction in fMLF-activated dHL-60 cells. dHL-60 cells were incubated with CLLV-1 (0.3–3 μM) for 5 min before stimulation with or without fMLF (0.1 μM)/CB (1 μg/mL). (a) The cell lysates were incubated with the thiol-alkylating agent AMS for 12 h on ice and analyzed by Western blotting under reducing (total lysate) or non-reducing conditions (AMS-labeled AKT). The AMS-labeled reduced form of AKT (Red) had a higher molecular weight than oxidized AKT (Oxi). (b) The cell lysates were immunoprecipitated with control (Ctrl) or AKT IgG. The precipitated substances were used for Western blotting of AKT and PP2A.

targets in AKT-associated disorders. In this study, CLLV-1 was found to be an allosteric inhibitor of AKT through covalently binding to Cys310 *in vitro* (Fig. 6). This is the first example of restraining neutrophilic inflammation by pharmacologically targeting the redox regulatory site of AKT. LPS-induced ALI is an important *in vivo* model to mimic clinical pulmonary destruction, such as pulmonary edema, alveolar-capillary barrier loss or inflammatory cell infiltration [38,40]. The novel covalent allosteric AKT inhibitor, CLLV-1, showed its anti-inflammatory effects to ameliorate LPS-primed ALI in mice, including neutrophils infiltration, pulmonary protease release, inter-alveolar septal thickening, interstitial edema, and AKT activation (Fig. 8). It proves the therapeutic potential for curing neutrophilic lung damage, ALI/ARDS, *via* pharmacological

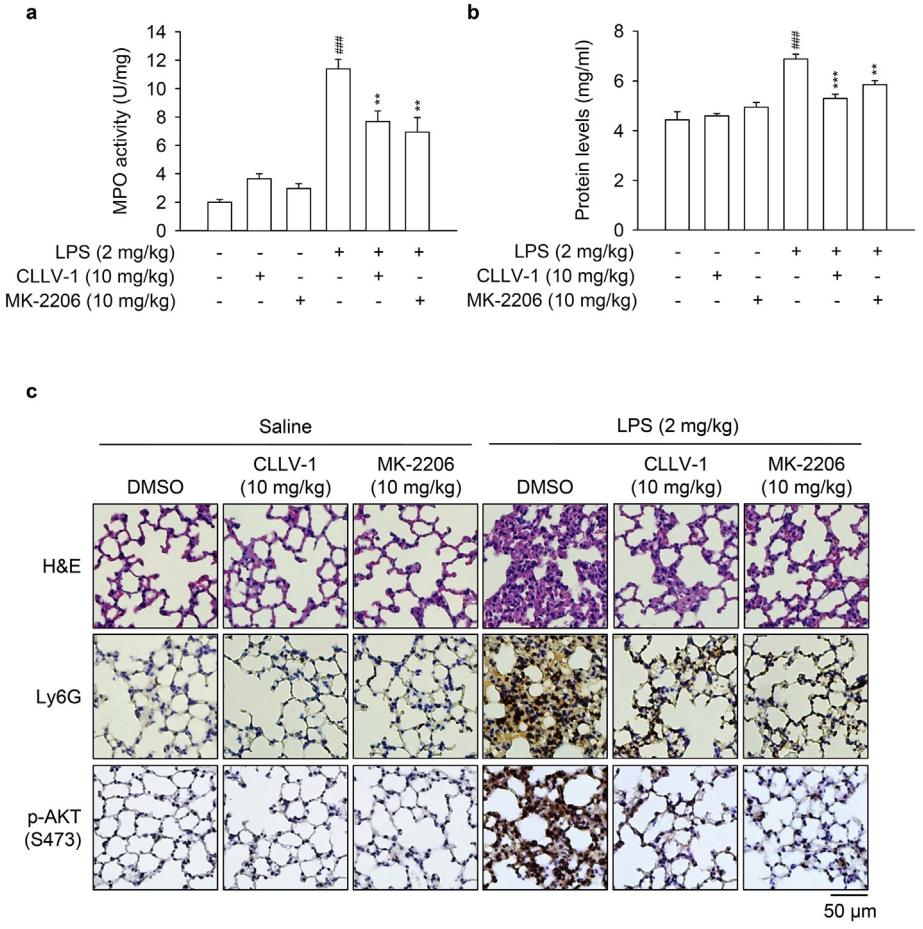

Fig. 8. CLLV-1 attenuates LPS-induced ALI in mice. C57BL/6 mice were intraperitoneally injected with CLLV-1 (10 mg/kg), MK-2206 (10 mg/kg), or an equal volume of DMSO for 1 h, and subsequently instilled 2 mg/kg LPS from *E. coli* 0111:B4 or 0.9% saline *via* tracheostomy. (a-b) Six hours later, lungs were collected and assayed for MPO activity (a) and protein levels (b). (c) Histological examination of lungs. The lung sections were stained with hematoxylin and eosin (H&E), anti-Ly6G antibodies, or anti-pAKT (S473) antibodies by IHC. All data are expressed as mean values ± SEM ($n = 6$); $^{**}p < .01$ and $^{***}p < .001$ compared with the LPS + DMSO group; $^{\#\#\#}p < .001$ compared with the DMSO control (Student's *t*-test).

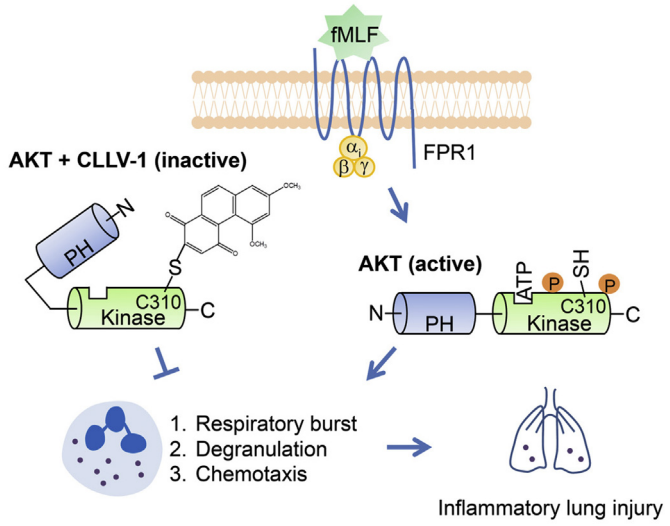

Fig. 9. Schematic model of CLLV-1-impeded neutrophilic inflammation. With stimulation, AKT is activated and phosphorylated, leading to the PH domain becoming more distant from the kinase domain. Active AKT is maintained in a reduced manner that contributes to overwhelming inflammatory responses in human neutrophils and neutrophil-dominant inflammatory disorders. Once CLLV-1 is administered, it covalently binds to Cys310 within the kinase domain of AKT, yielding an inactive and less reduced form of AKT. CLLV-1 can inhibit neutrophil activation, including respiratory burst, degranulation, and chemotaxis by modifying the redox state of AKT. Significantly, CLLV-1 ameliorates inflammatory ALI *in vivo*.

inhibition of AKT. Accordingly, anti-inflammatory drugs that target the redox modification of AKT could potentially be developed.

In summary, we demonstrate that AKT activation plays a critical role in neutrophilic lung injury. Targeting AKT Cys310 using drugs can regulate AKT enzymatic activity. Our findings also provide an important example of how a derivative of phenanthrenequinone, CLLV-1, restrains neutrophil-dominant inflammatory lung injury by inhibiting AKT activity in a redox-dependent manner (Fig. 9).

Funding sources

This research was financial supported by the grants from the Ministry of Science Technology (MOST 106-2320-B-255-003-MY3 and MOST 104-2320-B-255-004-MY3), Taiwan; Ministry of Education (EMRPD1G0231 and EMRPD1H0381), Taiwan; Chang Gung Memorial Hospital (CMRPF1F0011~3, CMRPF1F0061~3, CMRPF1G0241~3, and BMRP450), Taiwan. The funders had no role in study design, data collection and analysis, decision to publish, or preparation of the manuscript.

Declaration of interests

The authors declare that no competing interests exist.

Author contributions

P.J.C. and I.L.K. designed and performed most experiments. C.L.L., F.R.C., Y.C.W., Y.L.L., C.C.W., Y.F.T., C.Y.L., and C.Y.P. helped to perform experiments and analyzed the data. C.L.L., H.C.H., F.R.C., and Y.C.W. synthesized and provided CLLV-1. P.J.C. and T.L.H. wrote and completed the manuscript. T.L.H. supervised the entire study.

Appendix A. Supplementary data

Supplementary data to this article can be found online at https://doi.org/10.1016/j.ebiom.2019.01.043.

References

[1] Jorch SK, Kubes P. An emerging role for neutrophil extracellular traps in noninfectious disease. Nat Med 2017;23(3):279–87.
[2] Leiding JW. Neutrophil evolution and their diseases in humans. Front Immunol 2017;8:1009.
[3] Nauseef WM, Borregaard N. Neutrophils at work. Nat Immunol 2014;15(7):602–11.
[4] Mortaz E, Alipoor SD, Adcock IM, Mumby S, Koenderman L. Update on neutrophil function in severe inflammation. Front Immunol 2018;9:2171.
[5] Soehnlein O, Steffens S, Hidalgo A, Weber C. Neutrophils as protagonists and targets in chronic inflammation. Nat Rev Immunol 2017;17(4):248–61.
[6] Delano MJ, Ward PA. Sepsis-induced immune dysfunction: can immune therapies reduce mortality? J Clin Invest 2016;126(1):23–31.
[7] White MM, Geraghty P, Hayes E, Cox S, Leitch W, Alfawaz B, et al. Neutrophil membrane cholesterol content is a key factor in cystic fibrosis lung disease. EBioMedicine 2017;23:173–84.
[8] Rebetz J, Semple JW, Kapur R. The pathogenic involvement of neutrophils in acute respiratory distress syndrome and transfusion-related acute lung injury. Transfus Med Hemother 2018;45(5):290–8.
[9] Tsai YF, Yang SC, Hwang TL. Formyl peptide receptor modulators: a patent review and potential applications for inflammatory diseases (2012–2015). Expert Opin Ther Pat 2016:1–18.
[10] Yang SC, Hwang TL. The potential impacts of formyl peptide receptor 1 in inflammatory diseases. Front Biosci (Elite Ed) 2016;8:436–49.
[11] Liu J, Qian C, Cao X. Post-translational modification control of innate immunity. Immunity 2016;45(1):15–30.
[12] Weiss E, Kretschmer D. Formyl-peptide receptors in infection, inflammation, and cancer. Trends Immunol 2018;39(10):815–29.
[13] Zhang Y, Wang X, Yang H, Liu H, Lu Y, Han L, et al. Kinase AKT controls innate immune cell development and function. Immunology 2013;140(2):143–52.
[14] Manning BD, Toker A. AKT/PKB signaling: navigating the network. Cell 2017;169(3):381–405.
[15] Chamcheu JC, Adhami VM, Esnault S, Sechi M, Siddiqui IA, Satyshur KA, et al. Dual inhibition of PI3K/Akt and mTOR by the dietary antioxidant, delphinidin, ameliorates psoriatic features in vitro and in an imiquimod-induced psoriasis-like disease in mice. Antioxid Redox Signal 2017;26(2):49–69.
[16] Hoyal CR, Gutierrez A, Young BM, Catz SD, Lin JH, Tsichlis PN, et al. Modulation of p47PHOX activity by site-specific phosphorylation: Akt-dependent activation of the NADPH oxidase. Proc Natl Acad Sci U S A 2003;100(9):5130–5.
[17] El-Benna J, Dang PM, Gougerot-Pocidalo MA, Marie JC, Braut-Boucher F. p47phox, the phagocyte NADPH oxidase/NOX2 organizer: structure, phosphorylation and implication in diseases. Exp Mol Med 2009;41(4):217–25.
[18] Chen J, Tang H, Hay N, Xu J, Ye RD. Akt isoforms differentially regulate neutrophil functions. Blood 2010;115(21):4237–46.
[19] Nanamori M, Chen J, Du X, Ye RD. Regulation of leukocyte degranulation by cGMP-dependent protein kinase and phosphoinositide 3-kinase: potential roles in phosphorylation of target membrane SNARE complex proteins in rat mast cells. J Immunol 2007;178(1):416–27.
[20] Hoenderdos K, Lodge KM, Hirst RA, Chen C, Palazzo SG, Emerenciana A, et al. Hypoxia upregulates neutrophil degranulation and potential for tissue injury. Thorax 2016;71(11):1030–8.
[21] Kumar S, Xu J, Kumar RS, Lakshmikanthan S, Kapur R, Kofron M, et al. The small GTPase Rap1b negatively regulates neutrophil chemotaxis and transcellular diapedesis by inhibiting Akt activation. J Exp Med 2014;211(9):1741–58.
[22] Chodniewicz D, Zhelev DV. Novel pathways of F-actin polymerization in the human neutrophil. Blood 2003;102(6):2251–8.
[23] Ahmad F, Nidadavolu P, Durgadoss L, Ravindranath V. Critical cysteines in Akt1 regulate its activity and proteasomal degradation: implications for neurodegenerative diseases. Free Radic Biol Med 2014;74:118–28.
[24] Durgadoss L, Nidadavolu P, Valli RK, Saeed U, Mishra M, Seth P, et al. Redox modification of Akt mediated by the dopaminergic neurotoxin MPTP, in mouse midbrain, leads to down-regulation of pAkt. FASEB J 2012;26(4):1473–83.
[25] Corcoran A, Cotter TG. Redox regulation of protein kinases. FEBS J 2013;280(9):1944–65.
[26] Zeng T, Zhang CL, Zhao N, Guan MJ, Xiao M, Yang R, et al. Impairment of Akt activity by CYP2E1 mediated oxidative stress is involved in chronic ethanol-induced fatty liver. Redox Biol 2018;14:295–304.
[27] Lo HM, Hwang TL, Wu WB. A phenanthrene derivative, 5,7-dimethoxy-1,4-phenanthrenequinone, inhibits cell adhesion molecule expression and migration in vascular endothelial and smooth muscle cells. Pharmacology 2017;99(5–6):291–302.
[28] Lee CL, Lin YT, Chang FR, Chen GY, Backlund A, Yang JC, et al. Synthesis and biological evaluation of phenanthrenes as cytotoxic agents with pharmacophore modeling and ChemGPS-NP prediction as topo II inhibitors. PLoS One 2012;7(5):e37897.
[29] Chen PJ, Wang YL, Kuo LM, Lin CF, Chen CY, Tsai YF, et al. Honokiol suppresses TNF-alpha-induced neutrophil adhesion on cerebral endothelial cells by disrupting polyubiquitination and degradation of IkappaBalpha. Sci Rep 2016;6(6):26554.
[30] Yuan P, Temam S, El-Naggar A, Zhou X, Liu DD, Lee JJ, et al. Overexpression of podoplanin in oral cancer and its association with poor clinical outcome. Cancer 2006;107(3):563–9.
[31] Dorward DA, Lucas CD, Chapman GB, Haslett C, Dhaliwal K, Rossi AG. The role of formylated peptides and formyl peptide receptor 1 in governing neutrophil function during acute inflammation. Am J Pathol 2015;185(5):1172–84.
[32] Yang SC, Chen PJ, Chang SH, Weng YT, Chang FR, Chang KY, et al. Luteolin attenuates neutrophilic oxidative stress and inflammatory arthritis by inhibiting Raf1 activity. Biochem Pharmacol 2018;154:384–96.

[33] Futosi K, Fodor S, Mocsai A. Reprint of Neutrophil cell surface receptors and their intracellular signal transduction pathways. Int Immunopharmacol 2013;17(4):1185–97.
[34] Hirai H, Sootome H, Nakatsuru Y, Miyama K, Taguchi S, Tsujioka K, et al. MK-2206, an allosteric Akt inhibitor, enhances antitumor efficacy by standard chemotherapeutic agents or molecular targeted drugs in vitro and in vivo. Mol Cancer Ther 2010;9(7):1956–67.
[35] Weichhart T, Hengstschlager M, Linke M. Regulation of innate immune cell function by mTOR. Nat Rev Immunol 2015;15(10):599–614.
[36] Brazil DP, Yang ZZ, Hemmings BA. Advances in protein kinase B signalling: AKTion on multiple fronts. Trends Biochem Sci 2004;29(5):233–42.
[37] Sousa LP, Lopes F, Silva DM, Tavares LP, Vieira AT, Rezende BM, et al. PDE4 inhibition drives resolution of neutrophilic inflammation by inducing apoptosis in a PKA-PI3K/Akt-dependent and NF-kappaB-independent manner. J Leukoc Biol 2010;87(5):895–904.
[38] Tsai YF, Chu TC, Chang WY, Wu YC, Chang FR, Yang SC, et al. 6-Hydroxy-5,7-dimethoxy-flavone suppresses the neutrophil respiratory burst via selective PDE4 inhibition to ameliorate acute lung injury. Free Radic Biol Med 2017;106:379–92.
[39] Murata H, Ihara Y, Nakamura H, Yodoi J, Sumikawa K, Kondo T. Glutaredoxin exerts an antiapoptotic effect by regulating the redox state of Akt. J Biol Chem 2003;278(50):50226–33.
[40] Yang SC, Chang SH, Hsieh PW, Huang YT, Ho CM, Tsai YF, et al. Dipeptide HCH6-1 inhibits neutrophil activation and protects against acute lung injury by blocking FPR1. Free Radic Biol Med 2017;106:254–69.
[41] Yeh YC, Yang CP, Lee SS, Horng CT, Chen HY, Cho TH, et al. Acute lung injury induced by lipopolysaccharide is inhibited by wogonin in mice via reduction of Akt phosphorylation and RhoA activation. J Pharm Pharmacol 2016;68(2):257–63.
[42] Nicolas-Avila JA, Adrover JM, Hidalgo A. Neutrophils in homeostasis, immunity, and cancer. Immunity 2017;46(1):15–28.
[43] Kim K, Li J, Barazia A, Tseng A, Youn SW, Abbadessa G, et al. ARQ 092, an orally-available, selective AKT inhibitor, attenuates neutrophil-platelet interactions in sickle cell disease. Haematologica 2017;102(2):246–59.
[44] Dennehy MK, Richards KA, Wernke GR, Shyr Y, Liebler DC. Cytosolic and nuclear protein targets of thiol-reactive electrophiles. Chem Res Toxicol 2006;19(1):20–9.
[45] Mi L, Hood BL, Stewart NA, Xiao Z, Govind S, Wang X, et al. Identification of potential protein targets of isothiocyanates by proteomics. Chem Res Toxicol 2011;24(10):1735–43.
[46] Galli S, Antico Arciuch VG, Poderoso C, Converso DP, Zhou Q, Bal de Kier Joffe E, et al. Tumor cell phenotype is sustained by selective MAPK oxidation in mitochondria. PLoS One 2008;3(6):e2379.
[47] Luanpitpong S, Chanvorachote P, Nimmannit U, Leonard SS, Stehlik C, Wang L, et al. Mitochondrial superoxide mediates doxorubicin-induced keratinocyte apoptosis through oxidative modification of ERK and Bcl-2 ubiquitination. Biochem Pharmacol 2012;83(12):1643–54.
[48] Keane NA, Glavey SV, Krawczyk J, O'Dwyer M. AKT as a therapeutic target in multiple myeloma. Expert Opin Ther Targets 2014;18(8):897–915.
[49] Nitulescu GM, Margina D, Juzenas P, Peng Q, Olaru OT, Saloustros E, et al. Akt inhibitors in cancer treatment: the long journey from drug discovery to clinical use (Review). Int J Oncol 2016;48(3):869–85.
[50] Jacinto E, Lorberg A. TOR regulation of AGC kinases in yeast and mammals. Biochem J 2008;410(1):19–37.
[51] Weisner J, Gontla R, van der Westhuizen L, Oeck S, Ketzer J, Janning P, et al. Covalent-allosteric kinase inhibitors. Angew Chem Int Ed Engl 2015;54(35):10313–6.
[52] Nguyen T, Coover RA, Verghese J, Moran RG, Ellis KC. Phenylalanine-based inactivator of AKT kinase: design, synthesis, and biological evaluation. ACS Med Chem Lett 2014;5(5):462–7.
[53] Lee JY, Lee YG, Lee J, Yang KJ, Kim AR, Kim JY, et al. Akt Cys-310-targeted inhibition by hydroxylated benzene derivatives is tightly linked to their immunosuppressive effects. J Biol Chem 2010;285(13):9932–48.
[54] Shearn CT, Reigan P, Petersen DR. Inhibition of hydrogen peroxide signaling by 4-hydroxynonenal due to differential regulation of Akt1 and Akt2 contributes to decreases in cell survival and proliferation in hepatocellular carcinoma cells. Free Radic Biol Med 2012;53(1):1–11.